The following supplement accompanies the article

The NARCliM project: model agreement and significance of climate projections

Roman Olson, Jason P. Evans, Alejandro Di Luca, Daniel Argüeso

*Corresponding author: romanolson85.w@gmail.com

Climate Research 69: 209–227 (2016)

This supplementary material presents inter-annual variability in temperature and precipitation, multi-model mean changes for the near-future (2020–2039) from the present-day period (1990–2009) for the RCMs and the driving GCMs, as well as the inner domain model-by-model far-future (2060–2079) RCM projections. In addition, the effect of averaging of far-future precipitation results over GCM grids is discussed.

1. Inter-annual variability

Here, we present inter-annual variability of temperature and precipitation, as quantified by inter-annual standard deviation of the 1990–2009 AWAP observations. The AWAP observations have been interpolated onto the inner domain using nearest-neighbour interpolation prior to the analysis. For temperature, the largest standard deviations are observed in the inland areas (except the far north of the domain) in austral summer, with values reaching as high as 1.5°C (Fig. S1). The lowest variability is observed in austral winter, particularly along the east coast, and in the south. As expected, annual mean variability tends to be lower than seasonal variability, due to an averaging out of shorter-term sub-annual variability.

The pattern of the precipitation variability (Fig. S2) largely mirrors that of the mean precipitation field (Fig. 4). Annually, the values range from close to zero over the far western part of the domain to above 30 mm mo^{-1} over parts of the New South Wales (NSW) coast. Higher values are observed on seasonal time scales, particularly during the warm season.

We note that each RCM has its own internal variability, which may be considerably different from the observations.

2. Near-future temperature changes

RCMs generally project significant agreeing warming in the near-future (Fig. S3), with the results similar between the 2 domains. The warming is expected to be highest in austral spring (SON) and summer (DJF) over land but is still expected to be below 1°C. Smallest changes (<0.5°C) are expected in austral winter in NSW, Victoria, and parts of South Australia, with most models projecting non-significant change over parts of this region. The RCM changes are typically smaller than the driving GCMs, while the patterns are similar, including highest warming over land in summer (DJF). The highest multi-model mean summer warming in the GCMs exceeds 1.5°C in summer over parts of NSW and in the north-west corner of the domain. The GCM warming is significant agreeing everywhere across the domain.

3. Near-future precipitation changes

Most RCMs do not project significant seasonal precipitation changes in the near-future (Fig. S4). The results are similar between the domains, although the outer domain features more pronounced drying over parts of eastern Queensland in summer (DJF). The local-scale near-future seasonal modelled changes are lower than the range of internal climate variability (Fig. S2).

This pattern contrasts with significant winter (JJA) and annual mean drying in the south-west of the

domain in the driving GCMs. In summer (DJF) and annually, the GCMs also feature a significant disagreeing area in the Tasman Sea off the coast of NSW.

4. Inner domain model-by-model far-future annual-mean projections

Model-by-model variations in inner-domain, far-future annual mean temperature and precipitation changes are shown in Figs. S5 and S6, respectively. For land temperatures, ECHAM5 and CCCMA3.1 are the models with the greatest warming. Specifically, ECHAM5 R2 projects a change exceeding 3°C over parts of Queensland. Models also differ in their representation of changes to the Tasman Sea warming hotspot close the east coast of NSW and in the latitude and breadth of a slow warming belt over the Tasman Sea. The response of the Great Australian Bight also varies, with CSIRO-Mk3.0-driven simulations warming the least—below 1°C.

Considerable inter-model differences are also found for precipitation changes. Over land, MIROC3.2-driven simulations produce large areas of significant wetting, primarily in the north. We note that these models are already too wet compared to the observations (not shown). Over land, CCCMA3.1- and CSIRO-Mk3.0-driven runs exhibit areas of significant wetting and drying, respectively, while ECHAM5-driven RCMs project no significant changes. Over the ocean, models also disagree on the significant change areas. For example, RCMs forced by ECHAM5 and CSIRO-Mk3.0 place the Tasman Sea wetting spot to the south of the other models. In the rest of the simulations, the wetting areas are collocated with the warming hot spots.

5. Averaging of inner-domain far-future precipitation changes over GCM cells

The significance results of the RCMs and GCMs represent different scales because each GCM data point represents an average over a larger area than the RCMs. The internal variability of climate decreases with the increasing scale (Kirtman et al. 2013). Because the *t*-test statistic is inversely proportional to inter-annual standard deviation, we expect the same change to become more significant when averaged over larger scales. To test this effect, we average the inner-domain RCM far-future precipitation changes over a relatively high-resolution GCM scale grid (MIROC3.2 T106 grid). The GCM grid-averaged results are then re-projected onto the original RCM grid and compared to the original RCM output. In Table S1, we see increases in the % significant area in all cases (where at least 1% of the area is significant) as expected. This result suggests that averaging over a common grid does indeed increase significance areas.

However, the GCMs used to drive the RCMs are not on the same grid. They contain both location mismatches and a range of grid scales. This fact creates an outstanding question: what effect does the GCM grid mismatch have on the percentage of significant areas? To address this question, we interpolate the GCM precipitation changes (sampled at the high-resolution RCM grid using nearest-neighbour interpolation) to a common (MIROC3.2) GCM scale grid using a simple average over MIROC3.2 cells. The common-grid output is then re-projected onto the high-resolution RCM grid using nearest-neighbour interpolation and compared to the original output. As Table S2 shows, in most cases, the effect of the location mismatch is to decrease significant areas, both agreeing and disagreeing. The relationship between an original model grid and a common grid would affect whether the location mismatch would decrease significance areas in other studies. However, if our findings hold more generally, then the GCM comparison studies that use this method to interpolate GCM output to a common grid might be overestimating the regions with significant change. Further research using a larger sample of models and output variables is required to validate this hypothesis.

When the inner-domain RCM output is averaged over the cells of their driving GCMs, the results are influenced by a combination of the grid scale (which in our case tends to increase significance areas) and location mismatch (which in our case tends to decrease significance areas) effects. The averaged multi-model mean changes are plotted in Fig. S7. The locations of the significant areas are generally similar to the non-averaged RCM case (Fig. 8, Table S3). The extent of significant agreeing areas is not consistently affected by the averaging, whereas the significant disagreeing area appears considerably larger in austral winter, which propagates into the annual mean results.

Overall, when averaging RCM output over driving GCM cells, there are 2 opposing effects on the significance areas. First, increasing scale tends to increase significance areas. Second, the location

mismatch between different GCMs tends to decrease significance areas. The effects counteract one another so that the percentage of significant agreeing area is not consistently affected by the averaging. One caveat of this analysis is that here we ignore spatial features and consider all grid cells to be independent. However, the value and significance of a certain grid cell are not important in itself because only a feature expressed by several model grid cells has meaning.

Supplementary Tables

Table S1. Diagnostics for areas of significant change for RCM ensemble mean precipitation. The GCM grid used here is that of MIROC3.2 (~1.1°). Agreeing area overlap is calculated as the percentage of significantly agreeing area in the original RCM output that remains significantly agreeing once the output is averaged over the GCM cells. **Bold** values indicate that the averaging increases the significant area. Areas of <1% are grey

Season	**Original inner-domain RCM output**		**Inner-domain RCM output averaged over typical GCM cells**		**Agreeing area overlap (%)**
	% significant agreeing area	% significant disagreeing area	% significant agreeing area	% significant disagreeing area	
DJF	0.39	0.10	**1.4**	0.0	43
MAM	1.3	~0.0	**3.3**	0.0	58
JJA	12	6.3	**14**	**11**	80
SON	11	0.014	**14**	0.0	86
Annual	14	2.4	**19**	**2.9**	86

Table S2. Diagnostics for areas of significant change for multi-model mean GCM precipitation calculated on the RCM grid (~0.1°) using nearest neighbour interpolation. Agreeing area overlap is calculated as the percentage of significantly agreeing area in the original GCM output on the inner domain RCM grid that remains significantly agreeing once the output is averaged over the MIROC3.2 cells. **Bold** values indicate that the averaging increases the significant area. Areas of <1% are grey

Season	**Original GCM output sampled on the inner-domain RCM grid**		**GCM output averaged over typical GCM cells**	
	% significant agreeing area	% significant disagreeing area	% significant agreeing area	% significant disagreeing area
DJF	0.48	8.9	0.0	**11.0**
MAM	1.1	1.1	0.8	**1.2**
JJA	18	7.1	**24**	**12**
SON	20	0.0	**23**	0.0
Annual	12	6.5	9.9	**6.8**

Table S3. Diagnostics for areas of significant change for inner-domain RCM ensemble mean precipitation. Agreeing area overlap is calculated as the percentage of significantly agreeing area in the original RCM output that remains significantly agreeing once the output is averaged over the driving GCM cells. **Bold** values indicate that the averaging increases the significant area. Areas of <1% are grey

Season	**Original inner-domain RCM output**		**Inner-domain output averaged over driving GCM cells**		**Agreeing area overlap (%)**
	% significant agreeing area	% significant disagreeing area	% significant agreeing area	% significant disagreeing area	
DJF	0.39	0.10	0.31	**0.16**	22
MAM	1.3	~0.0	**3.0**	0.0	61
JJA	12	6.3	12	**10**	75
SON	11	0.014	**15**	**0.33**	85
Annual	14	2.4	13	**5.0**	75

Supplementary Figures.

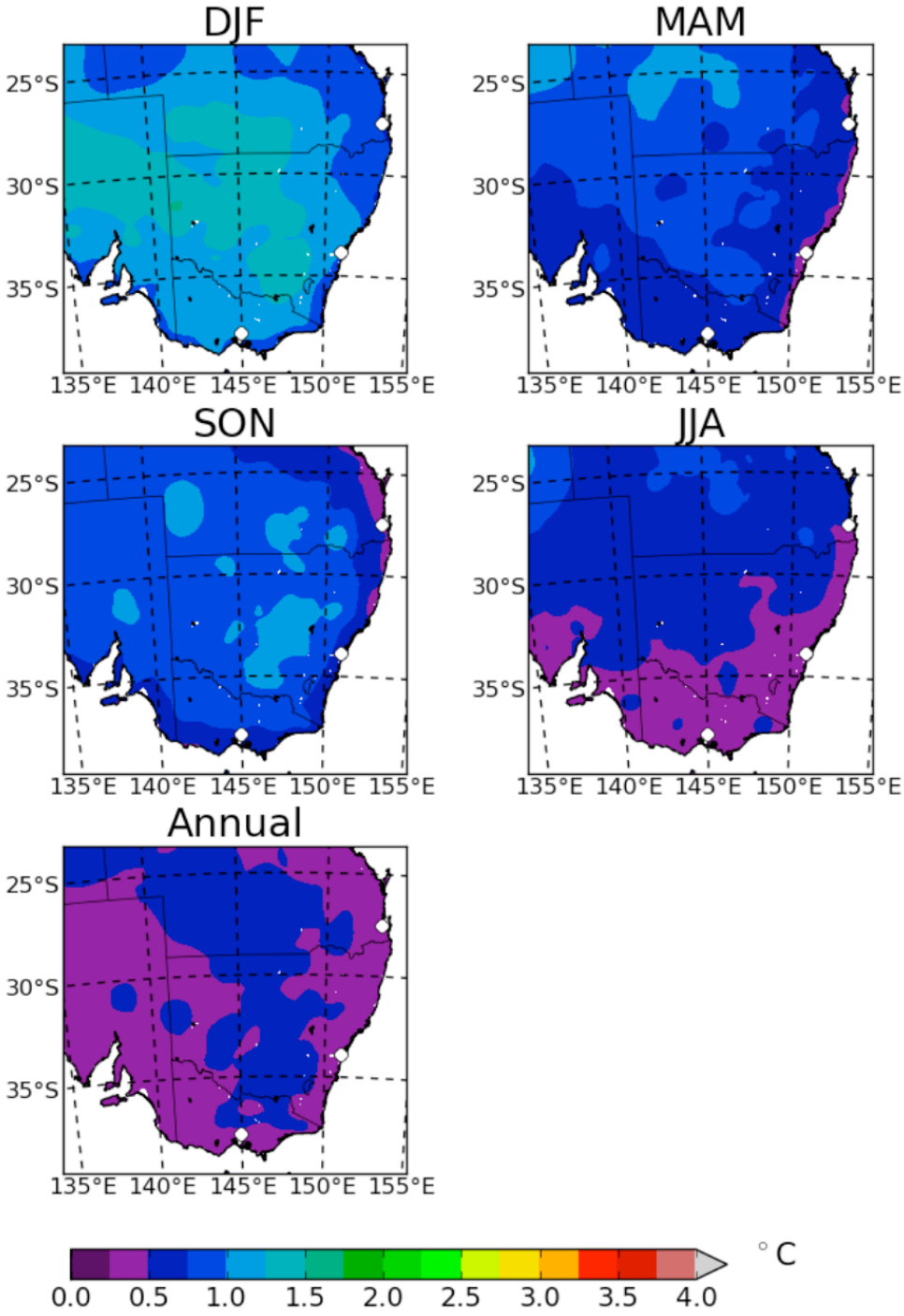

Fig. S1. Inter-annual standard deviation of seasonal and annual AWAP temperature observations for years 1990 to 2009 (°C). The observations have been interpolated to inner domain grid prior to analysis

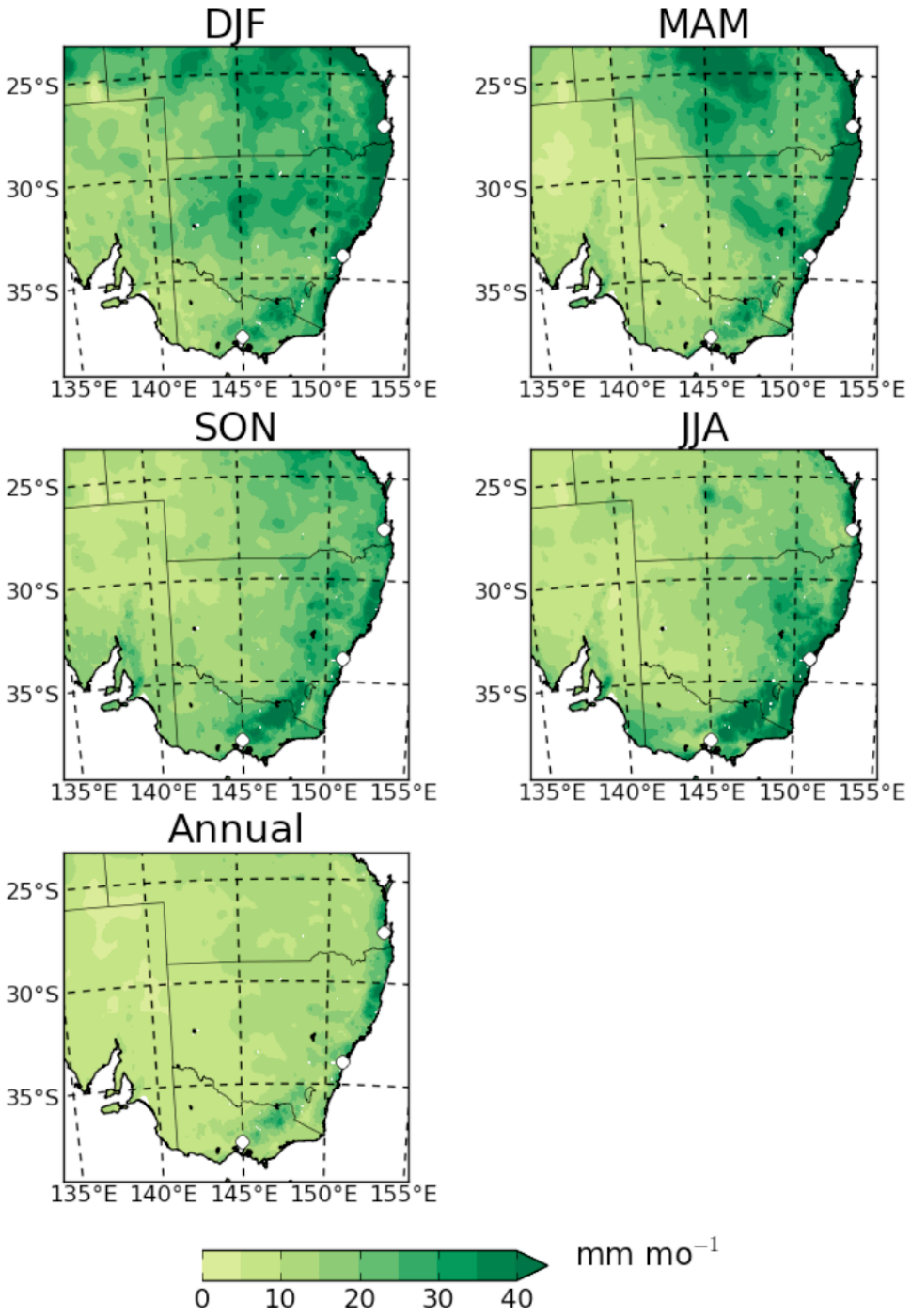

Fig. S2. Inter-annual standard deviation of seasonal and annual AWAP precipitation observations for years 1990 to 2009 (mm mo^{-1}). The observations have been interpolated to inner domain grid prior to analysis

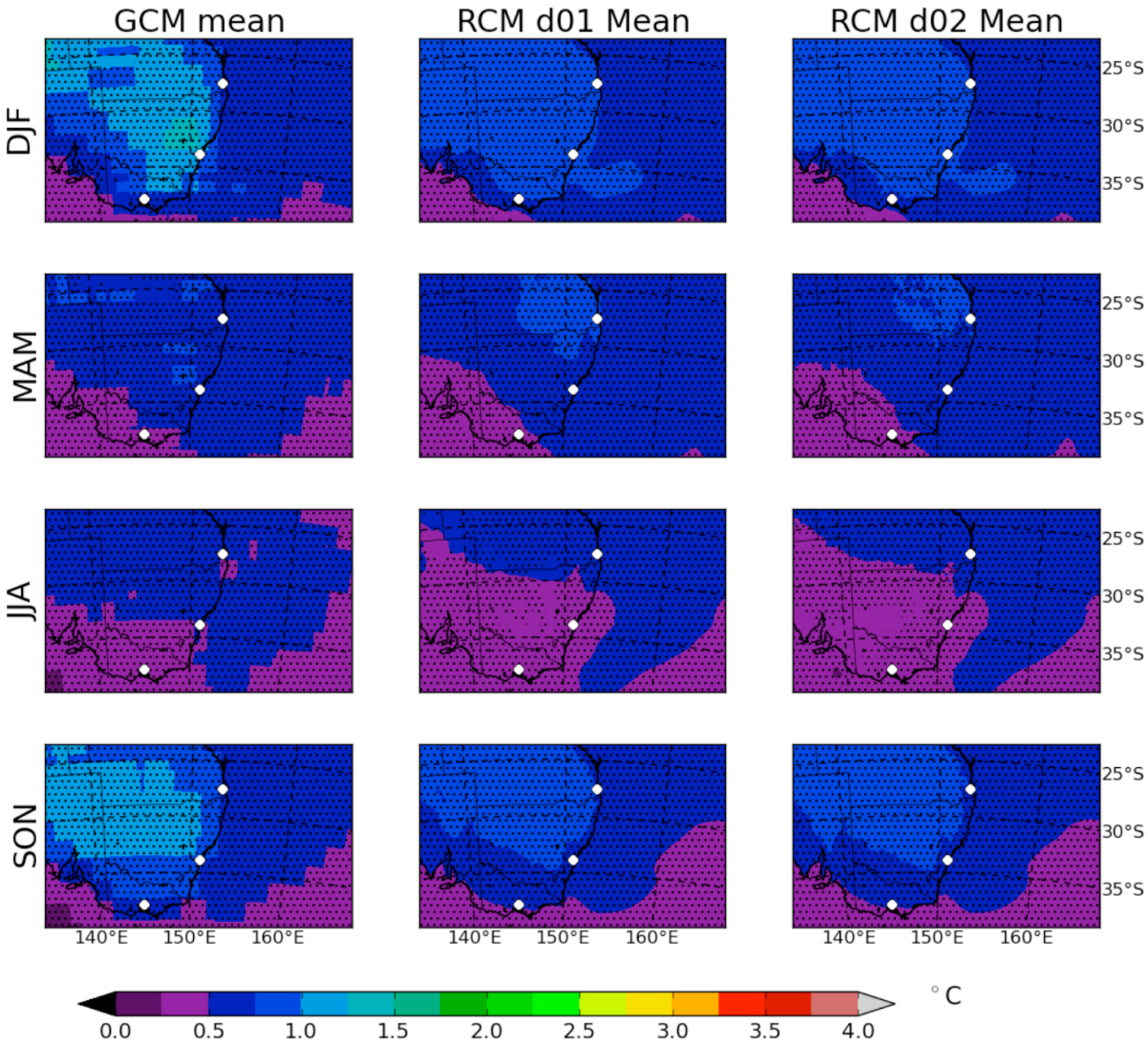

Fig. S3. Ensemble mean seasonal near-surface atmospheric temperature change from present day (1990–2009) to near future (2020–2039) (°C) for the GCMs, the RCMs on domain 01, and the RCMs on domain 02. Stippled (significant agreeing) areas indicate that half or more models show a statistically significant change, with 80% of more significant models changing in the same direction. White (significant disagreeing) areas indicate that half or more models show a statistically significant change, with less than 80% of significant models changing in the same direction

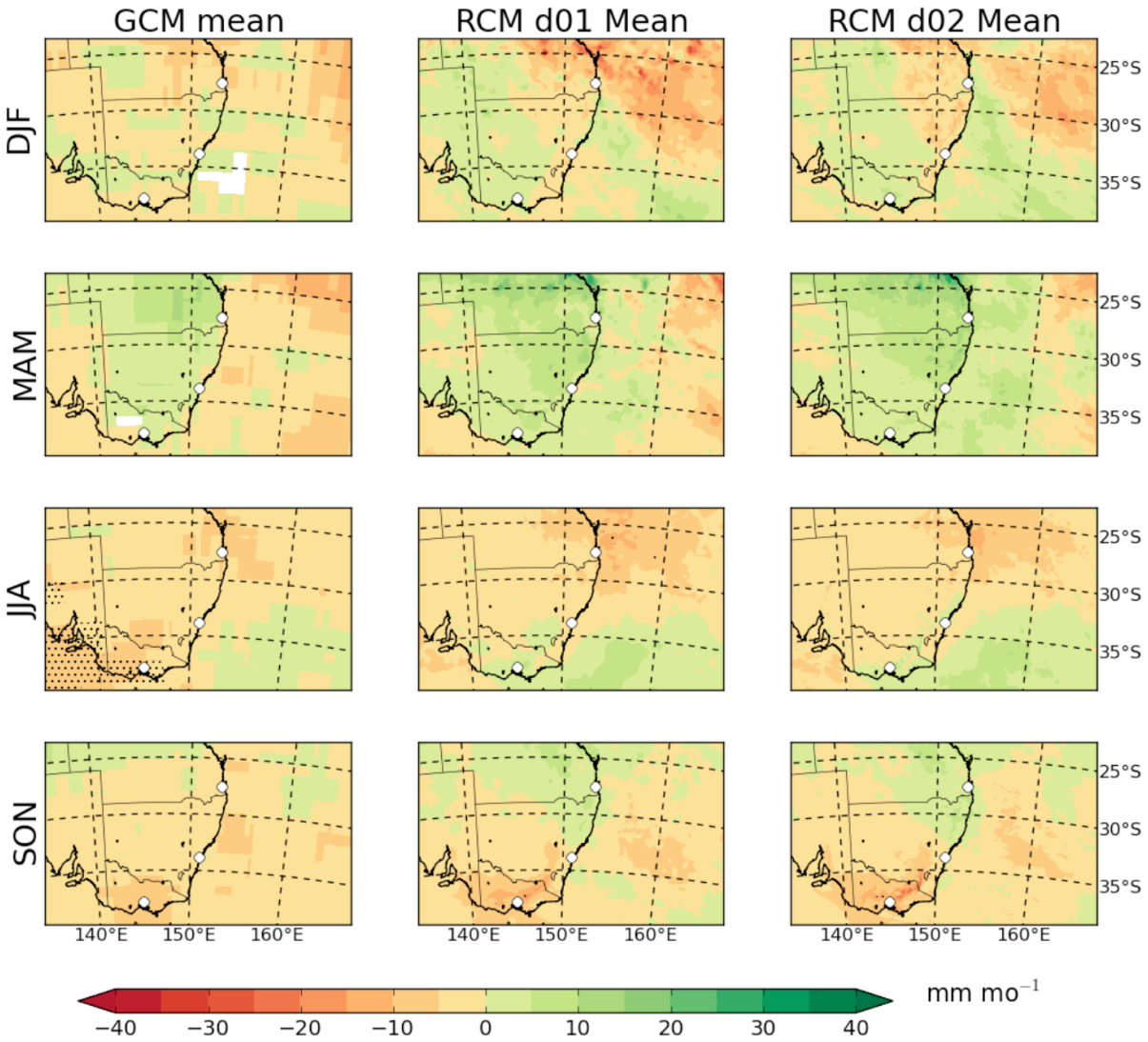

Fig. S4. Ensemble mean seasonal near-surface precipitation change from present day (1990–2009) to near future (2020–2039) (mm mo^{-1}) for the GCMs, the RCMs on domain 01, and the RCMs on domain 02. Stippling and white colouring convention as Fig. S3

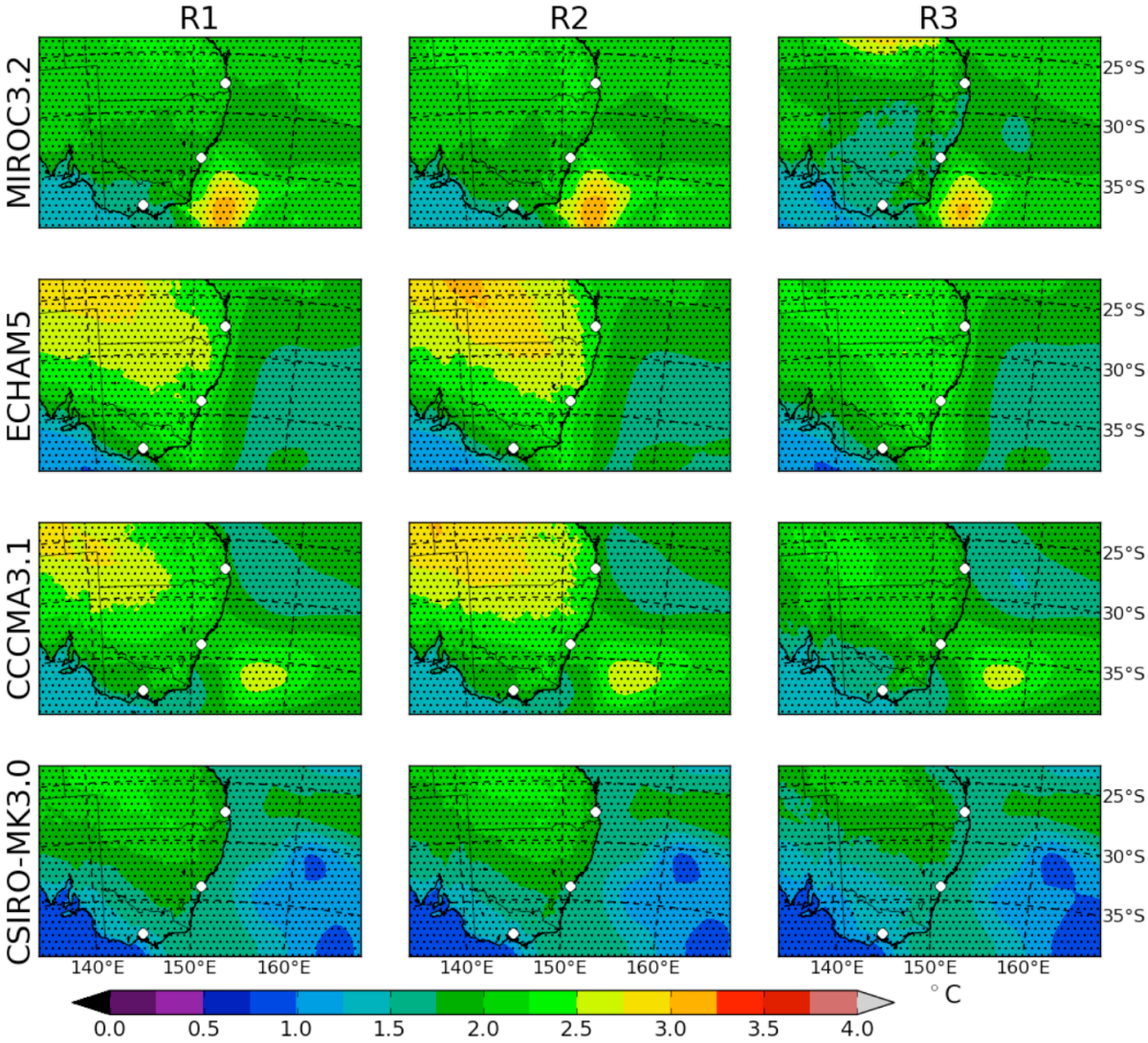

Fig. S5. Annual mean change between years 1990–2009 and 2060–2079 for near-surface air temperature (°C) for the inner domain RCMs. Stippled areas indicate statistical significance

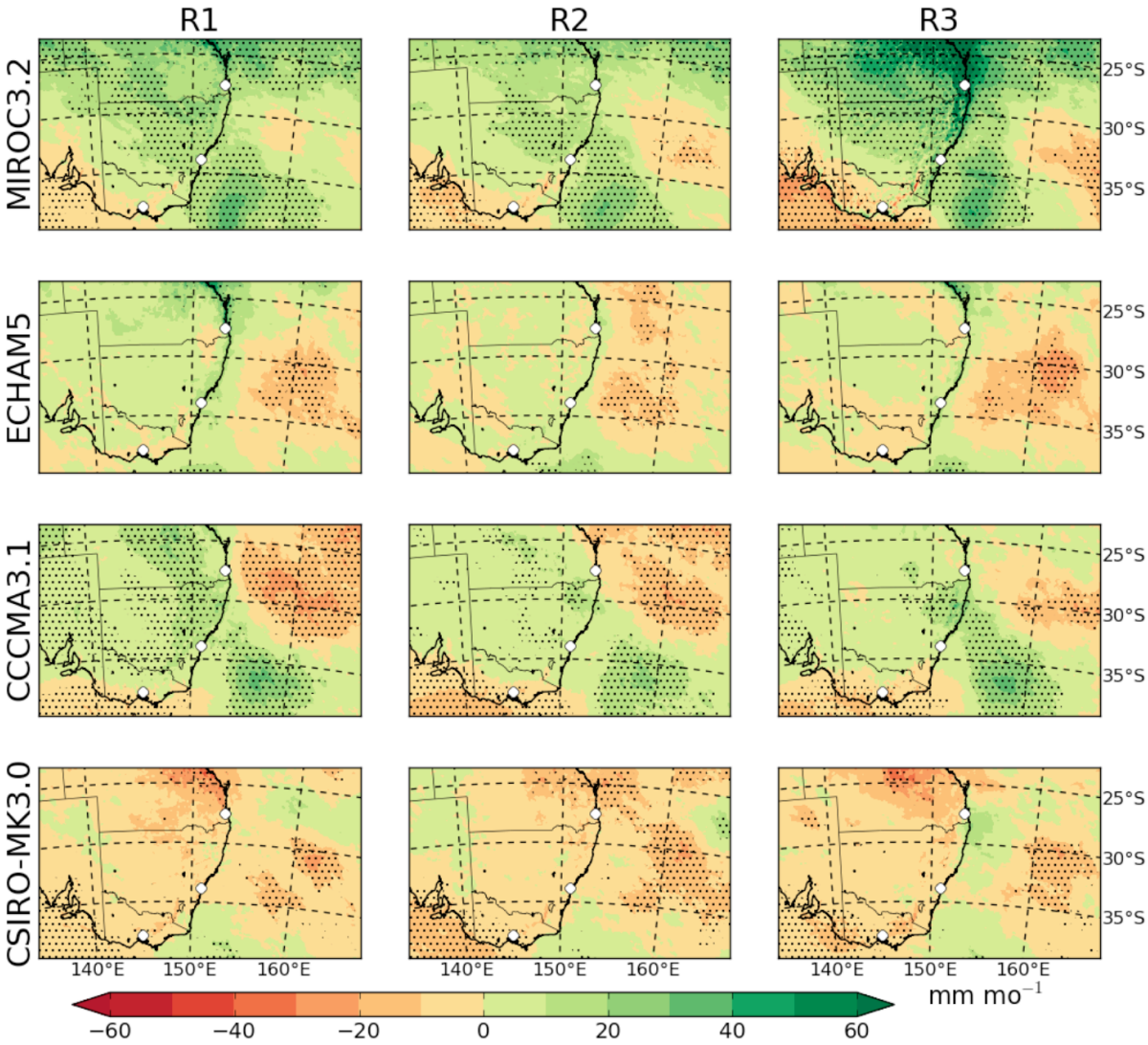

Fig. S6. Annual mean change between years 1990–2009 and 2060–2079 for precipitation (mm mo^{-1}) for the inner domain RCMs. Stippled areas indicate statistical significance

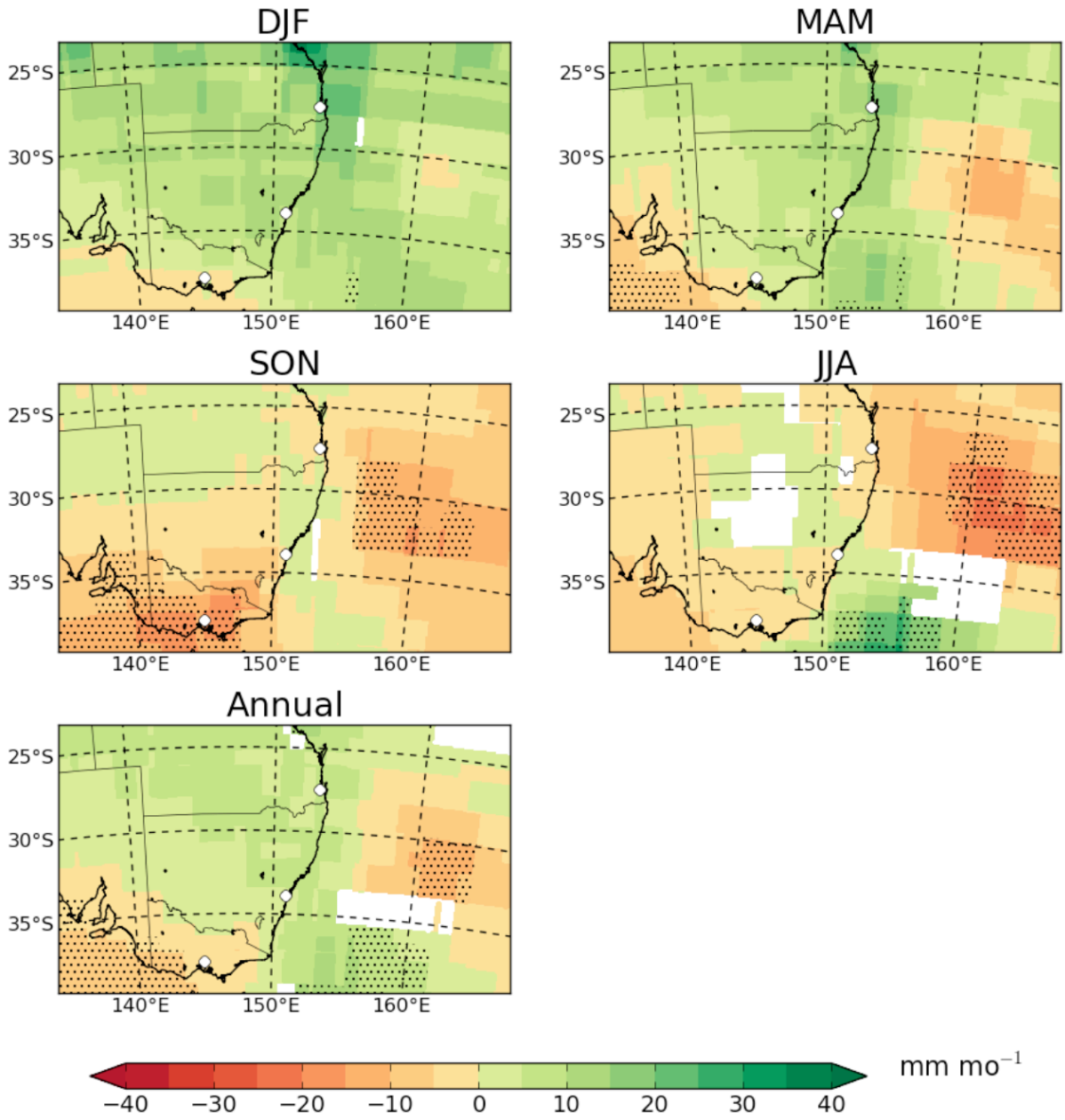

Fig. S7. Inner-domain RCM ensemble mean seasonal and annual precipitation change from present day (1990–2009) to far future (2060–2079) (mm mo^{-1}). The individual RCM precipitation was averaged over the cells of a corresponding driving GCM before taking the multi-model mean. Stippling and white colouring convention as in Fig. S3